

## Introduction

The rising cost of seismic acquisition and the proliferation of “exotic” geometries (wide azimuth, ocean-bottom node, 3D VSP) amplify the risk of making the wrong acquisition choices. The union of “full wave” computer simulation of 3D seismic surveys and prestack depth migration can greatly mitigate this risk. By reproducing the entire experiment as faithfully as possible, given the best prior information, seismic data consumers can confidently optimize survey geometry, long before expensive commitments are made.

Once a computationally intractable task, the simulation of 3D surveys has been almost fully commoditized, thanks to inexpensive Linux clusters. The key to maximizing the value of the simulated data lies in the imaging step. In this abstract, we present a flexible angle decomposition scheme for wave equation shot record migration. This innovation allows the construction of full-volume incidence angle gather, dip angle gathers, and azimuth angle gathers—with only a minor amount of overhead. Successful imaging is all about illumination, and angle decomposition gets to the core of the illumination problem.

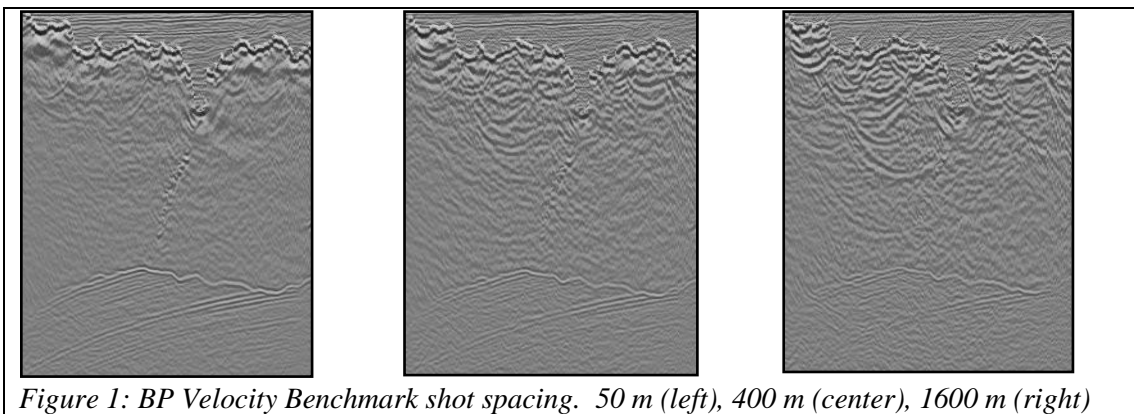
We present a case study using a “deepwater” adaptation of the SEG/EAGE Salt Model.

## Simulation and Imaging

The simulation and imaging concept is quite simple:

- Define an earth model containing appropriate reflectivity
- Define source positions and solve a wave equation in the earth model for each source
- Define geophone positions, save wavefield amplitude at all times to form shot records
- If appropriate, extract subset(s) of the dataset (example: narrow azimuth)
- Migrate dataset(s), load into workstation for comparison/analysis

The simulation step is generally the most computationally intensive aspect of the process. However, we have found that for the purposes of many simulation and imaging studies, especially when targets are deep, we can considerably decimate shot spacing relative to actual acquisition geometries without compromising the basic conclusions of the study. Figure 1 shows the result of migrating the BP Velocity Benchmark data with 50 m, 400 m, and 1,600 m shot spacing. The 50 m and 400 m results are largely similar, barring cosmetic considerations. The 1,600 m image suffers from a material loss of event focusing.



## Revisiting the “PI” in “PSPI”

Phase Shift Plus Interpolation (Gazdag & Squazzero, 1984) is a well-known method for solving the “one-way” factorization of the acoustic wave equation. Another work (Higginbotham, 2009), revisits the “plus interpolation” part of PSPI, mainly to put the algorithm on solid ground, because our angle decomposition scheme for wave equation shot record migration is intimately linked to the PSPI method.

In PSPI, the wavefield at depth  $z$  is efficiently downward continued to depth  $z+\Delta z$  using the phase shift method, for two or more constant velocities. The downward continuation is done in  $(k_x, k_y)$ , but the velocity model varies as a function of  $(x, y)$ . To resolve this domain inconsistency, two constant velocity wavefields, call them  $P_1$  and  $P_2$ , are interpolated in the space domain using a space-variable interpolation weight,  $\alpha$ , to form:

$$P_v = \alpha P_1 + (1 - \alpha) P_2 \quad (1)$$

It is shown that defining  $\alpha$  in terms of *slowness squared* ensures that the interpolated wavefield  $P_v$  satisfies the scalar wave equation at the current depth.

### Angle Decomposition Imaging Condition for PSPI Shot Record Migration

We present a method to compute the propagation direction of the source and receiver wavefield in shot record migration, enabling us to compute the incidence angle of a reflection, as well as its azimuth and dip angles. By defining angle “bins”, we can create these three types of angle gathers at every  $(x, y)$  in the image, for a nominal incremental cost.

Yoon & Marfurt (2006) presented a scheme for computing the propagation direction of a wavefield at a given  $(x, y, z)$  using the concept of the Poynting Vector. Theirs was a space-domain approach—here we present a methodology to accomplish a similar task, but operate in the Fourier domain. The shot record migration used is a PSPI algorithm. We use the concept of a “carrier signal” to map Fourier wavenumbers back to the space domain, where they are interpreted as propagation angles.

We begin with the scalar wave equation in the frequency-wavenumber domain:

$$\frac{\omega^2}{v^2} = k_x^2 + k_y^2 + k_z^2 \quad (2)$$

The wavenumbers  $k_x$ ,  $k_y$ , and  $k_z$  define the propagation direction of the wavefield which solves wave equation (2). The components of that unit vector,  $u_x$ ,  $u_y$ , and  $u_z$ , are:

$$u_x = \frac{v}{\omega} k_x; \quad u_y = \frac{v}{\omega} k_y; \quad u_z = \frac{v}{\omega} k_z \quad (3)$$

In downward continuation migration,  $k_z$  is a function of  $k_x$  and  $k_y$ . We use the fact, stemming from equation (2), that the vector  $[u_x, u_y, u_z]$  is a unit vector to compute  $u_z$  as a function of  $u_x$  and  $u_y$ . In PSPI, the solution to the one-way wave equation for variable velocity (call it  $P_v$ ) is cast as a space-variable interpolation between the constant-velocity wavefields which “bracket” the velocity at a given  $(x, y)$  (call them  $P_1$  and  $P_2$ ):

$$P_v = \alpha P_1 + (1 - \alpha) P_2 \quad (4)$$

The specific choice of the interpolation weight,  $\alpha$ , was discussed in the previous section. Assume that  $P_1$  and  $P_2$  have propagation direction vectors  $[u_{x,1}, u_{y,1}, u_{z,1}]$  and  $[u_{x,2}, u_{y,2}, u_{z,2}]$ , respectively.  $P_v$  has a propagation direction vector  $[u_{x,v}, u_{y,v}, u_{z,v}]$ . Create terms of the form:

$$u_{x,v} P_v = \alpha u_{x,1} P_1 + (1 - \alpha) u_{x,2} P_2 \quad (5)$$

By relating  $u_{x,1}$  and  $u_{x,2}$  through velocity and manipulating equation (5), we obtain:

$$\mathbf{u}_{x,v} \mathbf{P}_v = \mathbf{u}_{x,1} \mathbf{P}_v + (1 - \alpha) \mathbf{u}_{x,1} \frac{\Delta V}{V_1} \mathbf{P}_2 \quad \text{and} \quad \mathbf{u}_{x,v} \mathbf{P}_v = \mathbf{u}_{x,2} \mathbf{P}_v - \alpha \mathbf{u}_{x,2} \frac{\Delta V}{V_1} \mathbf{P}_1 \quad (6)$$

$\Delta v$  is defined as  $V_2 - V_1$ . Multiply the first equation (6) by  $\alpha P_v^*$  and the second equation (6) by  $(1 - \alpha) P_v^*$ , then add and divide by  $P_v P_v^*$  to obtain:

$$\mathbf{u}_{x,v} = \alpha \mathbf{u}_{x,1} + (1 - \alpha) \mathbf{u}_{x,2} + \alpha(1 - \alpha) \Delta V \left( \frac{u_{x,1} P_2}{V_1 P_v} - \frac{u_{x,2} P_1}{V_2 P_v} \right) \quad (7)$$

Division by zero is avoided because  $P_v P_v^*$  is nonzero for any  $P_v$  of interest. The last term of equation (7) is small in most cases. It is zero when  $\alpha=0, 1$ , or  $0.5$ . Therefore,

$$\mathbf{u}_{x,v} \approx \alpha \mathbf{u}_{x,1} + (1 - \alpha) \mathbf{u}_{x,2} \quad (8)$$

Relationships analogous to equation (8) apply to the other components of the propagation direction vector,  $u_{y,v}$  and  $u_{z,v}$ . Equation (8) is significant. It allows us to apply the same type of PSPI interpolation scheme to reconstruct each component of the propagation direction vector. As a final step, the vector  $[u_x, u_y, u_z]$  must be normalized to unit magnitude.

Unit propagation vectors are computed in the above fashion for both the source and receiver wavefields in shot record migration—call these vectors  $\mathbf{u}_s$  and  $\mathbf{u}_r$ , respectively. They have z-components of opposite sign and are defined at every  $(x,y)$  position at the current depth. The incidence, dip, and azimuth angles of a reflection are related to  $\mathbf{u}_s$  and  $\mathbf{u}_r$  as follows:

$$\text{Incidence angle } \phi: \tan \phi = |\mathbf{u}_s - \mathbf{u}_r|^* |\mathbf{u}_s + \mathbf{u}_r|^{-1} \quad (9)$$

$$\text{Dip angle } \alpha: \tan \alpha = |\mathbf{u}_{s,z} - \mathbf{u}_{r,z}|^* [(\mathbf{u}_{s,x} - \mathbf{u}_{r,x}) + (\mathbf{u}_{s,y} - \mathbf{u}_{r,y})]^{-1/2} \quad (10)$$

$$\text{Azimuth angle } \beta: \tan \beta = (\mathbf{u}_{s,y} - \mathbf{u}_{r,y})^* (\mathbf{u}_{s,x} - \mathbf{u}_{r,x})^{-1} \quad (11)$$

Finally, we summarize the algorithmic elements of our angle decomposition technique:

1. At each depth step, compute the unit propagation vector for each source and receiver PSPI wavefield, according to equation (3)
2. Modulate (multiply) each source and receiver PSPI wavefield by the components of the corresponding unit propagation vector—this yields six additional wavefields
3. Multiply modulated wavefields by the unmodulated wavefield's complex conjugate
4. Normalize the wavefields from step 3 above with magnitude squared of the unmodulated wavefield to compute the elements of the unit propagation vectors  $\mathbf{u}_s$  and  $\mathbf{u}_r$  via equation (8).
5. Normalize  $\mathbf{u}_s$  and  $\mathbf{u}_r$  to unit magnitude

The user defines a set of angle “bins”. The bins span a range of incidence angles, azimuth angles, and/or dip angles. For each  $(x,y)$ , steps 1-5 are performed, producing  $\mathbf{u}_s$  and  $\mathbf{u}_r$ , which allows us to define three angles via equations (9), (10), and (11). When the source and receiver wavefields are correlated, the result is placed into the appropriate bin.

## Examples

Figure 2 and Figure 3 illustrate the simulation and imaging methodology on a “deepwater” adaptation of the SEG/EAGE salt model. 1,764 full-azimuth split-spread shot records were simulated over the model, with a shot spacing of 320 m and maximum offset of 4,320 m in  $x$  and  $y$ . The angle decomposition imaging condition for shot record migration was run for

incidence angle only—bins of  $10^\circ$  width were defined. Close examination of Figure 2 shows that sub-salt reflectors (weak at best) have less than  $20^\circ$  of illumination. Long offsets may do little to solve this problem, due to critical angle effects. A high-effort narrow-azimuth subset was extracted from the full-azimuth survey by restricting crossline offset to 800 m. Figure 3 compares a sub-salt depth slice for the full-azimuth and narrow-azimuth migrations ( $0-60^\circ$ ) incidence angle stack. Somewhat surprisingly, the primaries on the narrow-azimuth image are about as well imaged as on the full-azimuth image; however, we notice a large amount of noise. The data have no multiples; the multiple-attenuating property of full-azimuth data could pay a large dividend in practice, but we must conclude that full-azimuth data did not “pay for itself” in this example.

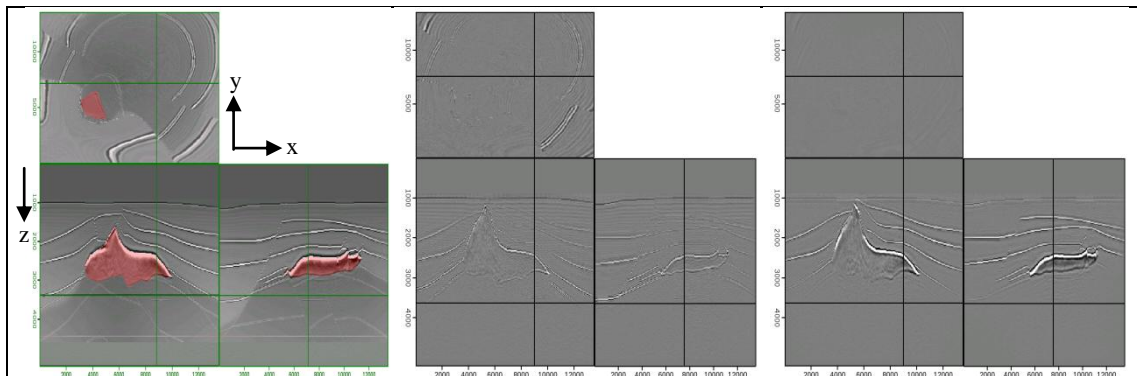


Figure 2: “Deepwater” SEG/EAGE model and full-azimuth images. Left:  $0-60^\circ$  incidence angle stack overlaying velocity model. Middle:  $0-10^\circ$  incidence angle stack. Right:  $20-30^\circ$  incidence angle stack.

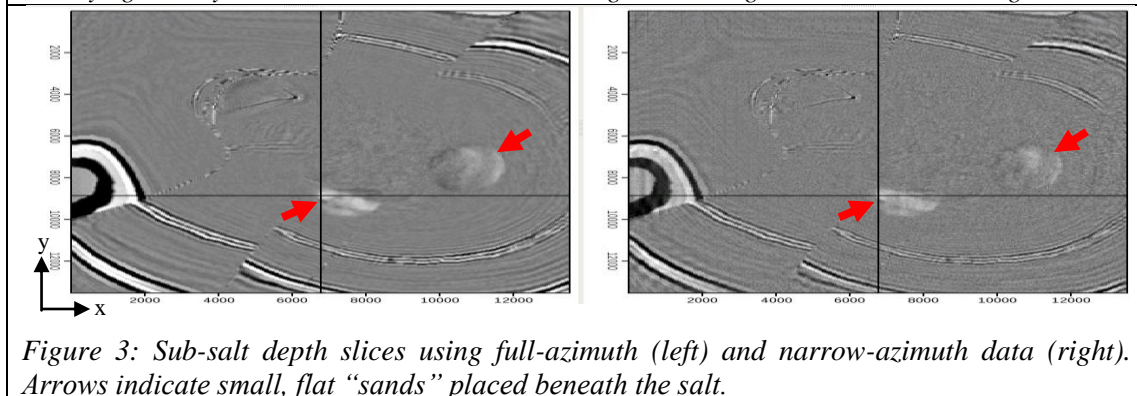


Figure 3: Sub-salt depth slices using full-azimuth (left) and narrow-azimuth data (right). Arrows indicate small, flat “sands” placed beneath the salt.

## Conclusions

Full wave simulation and imaging studies are within reach of nearly any E&P company—these studies have the potential to lead to significant improvements in pre-shoot decision making. We presented an angle decomposition scheme for wave equation shot record migration which allows us to dig even deeper into the illumination problem, producing full-volume gathers—incidence angle, azimuth angle, and/or dip angle. A sub-salt case study showed that full-azimuth data did **not** significantly improve illumination of the target zone.

## References

- Gazdag, J., & Squazzero, P. (1984). Migration of seismic data by phase shift plus interpolation. *Geophysics*, 49 (2), 124-131.
- Higginbotham, J. H. (2009). Revisiting the PI in PSPI. *SEG Annual Meeting*, (p. submitted).
- Yoon, K., & Marfurt, K. (2006). Reverse-time migration using the Poynting vector. *Exploration Geophysics*, 37 (1), 102-107.